nEDM: A Survey of Neutron Electric Dipole Moment Experiments

Scholarly paper submitted to the Graduate Committee of the

Department of Physics, University of Maryland at College Park

for the requirements for the Ph.D. candidacy

Advisor: Professor E. J. Beise

Thomas Langford

Abstract

This paper will cover a brief history of the search for the Neutron Electric Dipole Moment (nEDM). We will start with a theoretical introduction to the different processes which would yield an nEDM and the physical implications that it has to CP violation. This is followed by a survey of past and future experiments measuring nEDM. Specifically, it will cover the simulation method used to determine the sensitivity of the experiment to be run on the Spallation Neutron Source at Oak Ridge National Lab.

Contents

1 Introduction

Until 1950, the general belief was that charge conjugation, parity and time reversal were all good symmetries of nature. In a short letter to the editor of the Physical Review[1], E. M. Purcell and N. F. Ramsey made the argument that this belief was not based soundly upon experimental data. They suggested that a precision measurement of the static electric dipole moment of a fundamental particle would be a good test of these symmetries. Their argument was simple: the dipole moment must be aligned along its spin axis, since the particle has no other specified direction. However, spin is parity even, since it is an axial vector, and the electric dipole moment, $\vec{d} = e\,\vec{x}$, is parity odd. Thus the dipole moment would be aligned with the spin in one system, while in another it would be anti-aligned. Therefore the dipole moment must be zero for parity to be conserved. The same argument applies to time reversal asymmetry. Under time reversal, the spin changes direction, while the dipole moment remains unchanged. This can been seen in Figure 1.

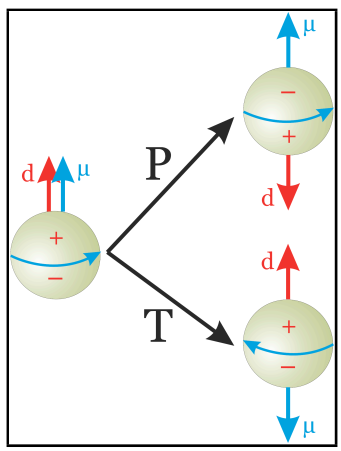

Figure 1: Magnetic and Electric Dipole Moments transforming under P and T.

The electric dipole moment of an elementary particle can be defined by a slight asymmetry in the charge distribution of the particle. In a charged particle this would relate to small deviation in the assumed uniform charge distribution. However, in a neutral particle, it would manifest as a small amount of positive charge in one half and an equal and opposite negative charge on the opposite half of the particle.

While there have been many advances in showing that these symmetries are not all good symmetries of different systems (including kaons and B mesons) the combined, CPT, symmetry is still held to be universal. As David Griffiths says in his book on Elementary Particles, "The [CPT] theorem is on extremely firm ground theoretically, and it is relatively secure experimentally. Indeed, as one prominent theorist put it, if a departure is ever found, 'all hell breaks loose.' " [2]

2 Theory of nEDM

2.1 Motivation - Baryon-Antibaryon Asymmetry

One of the large outstanding questions regarding the origin of the universe is the imbalance between matter and anti-matter. The problem lies in how matter was created in the Big Bang. Normally baryon and lepton numbers are conserved, so that when you create an electron, you also create a positron. There must have been a breaking of this symmetry to generate the universe seen today, with an abundance of matter, and a dearth of antimatter [3]. Sakharov first proposed calculating the baryon asymmetry. In doing so he noted three requirements to yield a baryon asymmetry from an initial state of $B = 0$ [4]:

1. Baryon number violation
2. CP violation
3. Departure from thermal equilibrium

If all three criteria are met, then the current asymmetry can be explained. However, although CP violation has been discovered in certain systems, there is currently not *enough* to explain the level of baryon-antibaryon asymmetry in the universe.

2.2 CP Violation in the Standard Model

CP violation was first discovered in the neutral kaon system by Cronin, et al.[5]. The experiment showed that the long-lived component of the neutral kaons, K_L^0, did, in fact, decay into two charged pions, thus violating CP. The K_L^0 has $CP = -1$ while the charged pions have $CP = 1$. Cronin and his colleagues were awarded the Nobel Prize in 1980 for their discovery.

There are two places where CP violation can be included in the Standard Model Lagrangian. One is ~~the~~ in the QCD ~~Theta~~ term and the other is the phase δ in the Cabibbo-Kobayashi-Maskawa (CKM) matrix which describes flavor mixing in the charged current interaction:

$$\begin{pmatrix} \overline{u} & \overline{c} & \overline{t} \end{pmatrix} \begin{pmatrix} c_1 & s_1 c_3 & s_1 s_3 \\ -s_1 c_2 & c_1 c_2 c_3 - e^{i\delta} s_2 s_3 & c_1 c_2 s_3 + e^{i\delta} s_2 c_3 \\ s_1 s_2 & -c_1 s_2 c_3 - e^{i\delta} c_2 s_3 & -c_1 s_2 s_3 - e^{i\delta} c_2 c_3 \end{pmatrix} \begin{pmatrix} d \\ s \\ b \end{pmatrix} \tag{1}$$

Here $c_i = \cos\theta_i$ and $s_i = \sin\theta_i$ with $\theta_i(i = 1, 2, 3)$ are the mixing angles. Working out the coupling constants and other theory intensive calculation, the Standard Model predicts:

$$d_n = -eG^2 sin\delta\, s_1 s_2 s_3 c_2 \frac{\alpha_s}{\sqrt{2}27\pi^3} \ln \frac{m_t^2}{m_c^2} \frac{f_\pi m_\pi^4}{m_s(m_u + m_d)} A(2\alpha - 1) g_A \ln \frac{m_K}{m_\pi}. \tag{2}$$

Assuming presently determined values for all these constants yields an estimate for the nEDM [6]:

$$d_n \approx 10^{-32} - 10^{-31} \text{ ecm}. \tag{3}$$

Which is still five orders of magnitude below the current experimental upper limit of nEDM.

2.3 Strong θ Problem in Quantum Chromodynamics

It is possible to introduce a CP violating term into the QCD Lagrangian by including the term:

$$L_\theta = -\theta \frac{\alpha_s}{8\pi} \tilde{G}^a_{\mu\nu} G^a_{\mu\nu}. \tag{4}$$

This is the so called “Theta Term.” Working in the chiral limit, $m_\pi \to 0$, we can express the leading order contribution to the nEDM as seen in Figure 2.

The CP violating, grey, vertex in the diagram is given by:

$$\overline{g_{\pi nn}} = -\theta \frac{m_u m_d}{m_u + m_d} \frac{\sqrt{2}}{f_\pi} \frac{M_\Xi - M_\Sigma}{m_s} \approx -0.027\theta. \tag{5}$$

Where ~~the~~ m_u, m_d, m_s are the masses of the up, down, and strange quarks; ~~the~~ M_Ξ and M_Σ are

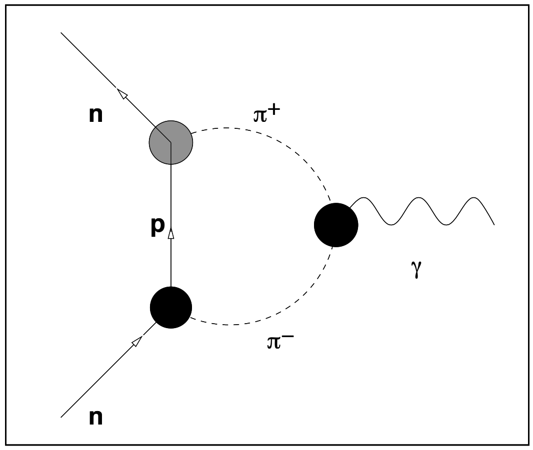

Figure 2: The mechanism of generating the nEDM. The grey vertex is the CP Violating $\pi^+ np$ vertex, while the two black circles are the normal CP conserving hadronic vertices [7]

.

the masses of the Ξ and Σ hyperons respectively; and f_π is the pion decay constant.

The diagram yields a nEDM of

$$d_n = \frac{e}{m_p} \frac{g_{\pi nn} \overline{g_{\pi nn}}}{4\pi^2} \ln \frac{m_p}{m_\pi}. \tag{6}$$

We can use this equation, combined with the fact that $g_{\pi nn} = 13.6$ is well known~~,~~ [8, 9], and the measured upper limit for d_n to obtain a value for θ:

$$|\theta| < 3 \times 10^{-10}. \tag{7}$$

There is no apparent reason for θ to be so small. The term was expected to be of order unity when first introduced into the Lagrangian. This is referred to as the "Strong Theta Problem" or the "Strong CP Problem." For a full discussion see ~~R~~eferences [6, 7].

There have been efforts to find a broken symmetry that would lead to the fine tuning of ~~theta~~. In particular, the Peccei-Quinn symmetry would invoke a global $U(1)$ symmetry that is spontaneously broken. However, this theory demands axions, which have thus far not been observed [3].

2.4 Neutron Electric Dipole Moment: Beyond the Standard Model

There have been a number of models looking beyond the Standard Model that have predictions for the Neutron Electric Dipole Moment. Continued experimental work on the measurement has led to the elimination of some of these models. Currently, there are Supersymmetric and Supergravity theories which will be tested by the next generation of experiments. For more on SUSY, specifically Left-Right Symmetric Models, see references [10, 11]. Similarly, a good overview of Supergravity can be found in reference [12].

3 Past nEDM Experiments

The past 50 years have seen an improvement of six orders of magnitude in the upper limits placed upon the neutron electric dipole moment. The progress can be seen in Figure 3. Current experiments are beginning to test Supersymmetric predictions, which has increased interest in the projects.

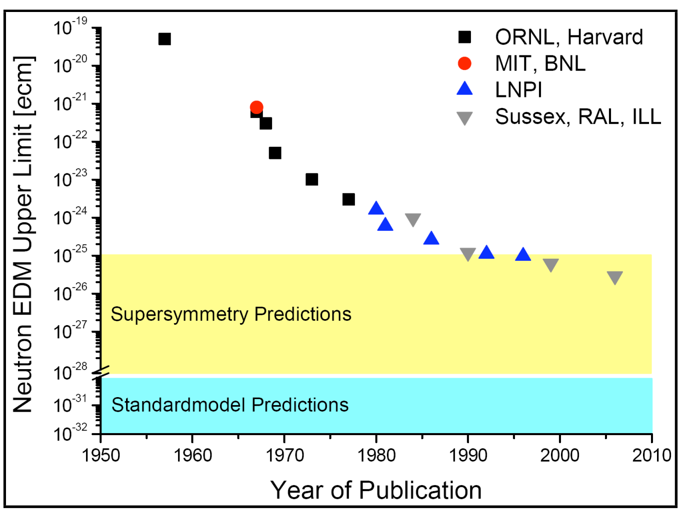

Figure 3: Upper limits placed on nEDM over the last 50 years.

3.1 Smith, Purcell and Ramsey, 1957

The first direct measurement of the nEDM was made on a thermal neutron beam produced by a reactor at Oak Ridge National Lab in 1950 by Smith, Purcell and Ramsey. ~~Though~~ the authors

~~felt~~ that any fundamental particle would provide a test of CP and P symmetries, the neutron was chosen because it lacks charge. The neutrality enabled a large electric field to be applied to the beam without changing its trajectory. This is one of the biggest advantages of studying the EDM of the neutron over other fundamental particles.

The resulting measurement was in accordance with Parity conservation and Time Reversal symmetry. Therefore Smith *et al.* initially decided not to publish their null results due to the scientific community's firm belief in C, P and T symmetries.

However, when Lee and Yang hypothesized [13], and Wu et al. subsequently found ~~[14],~~ evidence of Parity violation in beta decay, the community began to shift their views on the long held belief in C, P and T invariance. The results of Smith et al. were first published in ~~the~~ Physical Review in 1957~~.~~ [15] Their uncertainty placed an upper limit on the dipole moment of 5×10^{-20} e cm (90% C.L).

The experiment made use of Ramsey's Method of Separated Oscillatory Fields [6], a multi-step procedure for monitoring the precession frequency of neutrons. If the neutron has an EDM, the Larmor frequency (ν_L) – the frequency at which the spin of the neutron precesses in a magnetic field – will be shifted in the presence of an external electric field. If the Larmor frequency is well-known, the experiment can be set up to look for ~~any~~ deviation from the known frequency.

Ramsey's Method is ~~enumerated~~ here, heavily borrowed from *CP Violation Without Strangeness* by Khriplovich and Lamoreaux [6]. This assumes a coordinate system which places the ~~z~~ axis in the vertical direction and the ~~x-y~~ plane in the horizontal direction.

1. Polarize the neutrons in the z direction
2. Apply a $\pi/2$ pulse to rotate the spins into the x direction
3. Allow the spin to precess, in the $x - y$ plane, around a weak magnetic field in the z direction.
4. After a set period of time, such that $T = \frac{n}{\nu_L}$, apply a second $\pi/2$ pulse rotating the x component of the spin into the $-z$ direction. ~~Note that if~~ there is any deviation from the Larmor frequency, which would be caused by an EDM, there will be some component of the spin in the y direction. This is lost when the RF pulse is applied. Therefore the spin analyzer

measures ~~fewer neutrons polarized~~ in the z direction. This measurement can be taken to study any $\Delta\omega$ caused by an EDM interacting with an electric field.

The radio frequency magnetic field is applied near the resonant frequency of the neutron's precession. Scanning frequencies around the resonance shown in Figure 4, Smith et al. were able to verify that the $\pi/2$ pulse was applied properly. The measurements were then made as close to the peak as possible.

Smith et al. made use of this method for their beam-based experiment. Their experimental setup is seen in Figure 5. Since the neutrons are moving, the length of the apparatus is set by their velocity. The apparatus must be long enough to allow the neutrons to spend a substantial amount of time in the electric field. However, it must also be tuned to the Larmor frequency, so that the neutrons will precess by a known angle.

One of the main features of the setup is the neutron polarizer. This experiment is not possible without a good source of polarized neutrons. To achieve the necessary polarization, Smith et al. used a highly polished mirror made of iron, and placed it in a strong magnetic field. The field "saturates" the metal by aligning the ~~spin~~ of all the iron nuclei. The neutrons have a spin dependent cross section, so that the beam will separate into two; one that is polarized spin up, and one that is polarized spin down. The concept is similar to the Stern-Gerlach apparatus, ~~though~~ the implementation differs. The neutron mirror was used in a number of beam based experiments which followed.

As the beam based experiments progressed, some of their limitations became evident. First, since the beam ~~is~~ from a reactor, not all of the neutrons ~~are~~ traveling at the same velocity. This ~~makes~~ timing both $\pi/2$ pulses difficult, since the pulse ~~is dependent~~ ~~upon~~ the time spent in the radio frequency field. Second, the neutrons were thermal, with an average velocity of approximately 2000 m/s. This made precision electronics which could handle the fast switching of fields a priority. The final result obtained on a neutron beam in 1977 was $d_n = (0.4 \pm 1.5) \times 10^{-24} e\ cm$. This ~~placed~~ an upper limit of $d_n < 3 \times 10^{-24} e\ cm$ (90% confidence level) ~~on the nEDM~~. After 20 years of experiments, the systematic errors overwhelmed the counting statistics and a new method was needed [6].

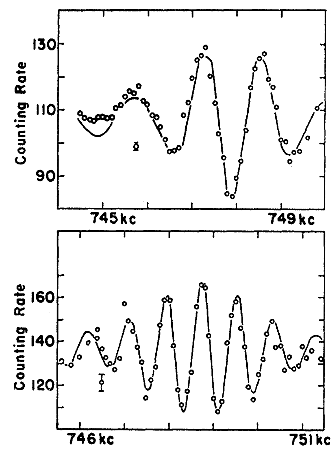

FIG. 2. Resonance curves of the neutron counting rate *versus* the frequency of the radio-frequency magnetic field. The upper curve is for a mirror angle of 3.14×10^{-3} radian, and the lower for 5.77×10^{-3} radian. A typical root-mean-square counting statistical error is shown. The lower curve shows a narrower resonance due to the fact that only slower neutrons are reflected at the larger mirror angles. It also shows more resonance detail since the polarized neutrons are more nearly monochromatic. The central peak is a minimum in the upper curve and a maximum in the lower curve since the phase of one of the coils was reversed.

Figure 4: Taken from Smith et al [15].

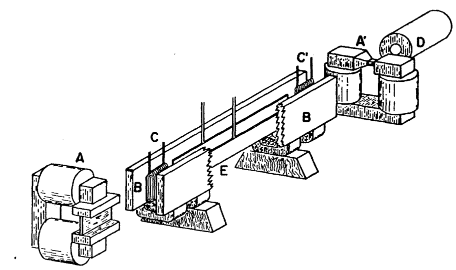

FIG. 1. Schematic diagram of the apparatus. A, the magnetized iron mirror polarizer. A', the magnetized iron transmission analyzer. B, the pole faces of the homogeneous field magnet. Note the horseshoe-like magnets bolted along the bottom. C, C', the coils for the radio-frequency magnetic field. D, the BF_3 neutron counter. The magnetic fields in the polarizing magnet and the homogeneous field magnet are at right angles, and two twisted iron strips were used between them to rotate the neutron spins adiabatically.

Figure 5: Taken from Smith et al [15].

3.2 Ultra Cold Neutron Based Experiments

The next big leap forward came with the ability to store neutrons. The idea has been attributed to Fermi, however the first article to suggest neutron storage was in 1959 by ~~a Russian scientist,~~ Yakov Zeldovich [16]. If the neutrons could be slowed to the point where their energy is less than the barrier potential from a surface, it could be possible to capture and store neutrons. The typical potential from a material barrier is $U_F \approx 200\ neV$, therefore the neutrons ~~have to~~ have velocities around 5 m/s to be stored. Such neutrons are referred to as Ultra Cold Neutrons (UCN).

It was also discovered that a new method of polarization was possible with UCNs. By adjusting the ratio of Fe to Co in a thin foil, it is possible to only transmit one spin state. By magnetically saturating the foil, the magnetic and effective potentials cancel for one spin state, while doubling the other. This leads to one spin state being totally reflected and the other being, effectively, completely transmitted. By having a higher polarization efficiency, the sensitivity of the experiment can be improved [6].

UCNs ~~have~~ become the new standard in nEDM searches. But ~~they also~~ have provided new means to test other properties of the neutron. Currently there are experiments using UCNs to measure the lifetime of the neutron to greater precision [17, 18]. ~~There has been great interest in measuring certain quantities to search for asymmetries, which would also provide interesting probes of the Standard Model. One of these is the radiative decay of the neutron, which involves measuring the branching ratio of~~ $\cancel{n \to e^- p\gamma}$ ~~[19].~~

Currently there are several collaborations working to make an improved measurement of the neutron electric dipole moment using UCNs. These include groups at ILL, the Paul Scherrer Institut in Switzerland and the Spallation Neutron Source (SNS) located at Oak Ridge National Lab (ORNL). ~~We will~~ focus on the ILL and ORNL experiments ~~for this paper~~.

3.2.1 Cryo-nEDM Experiment at Institute Laue-Langevin, Grenoble, France

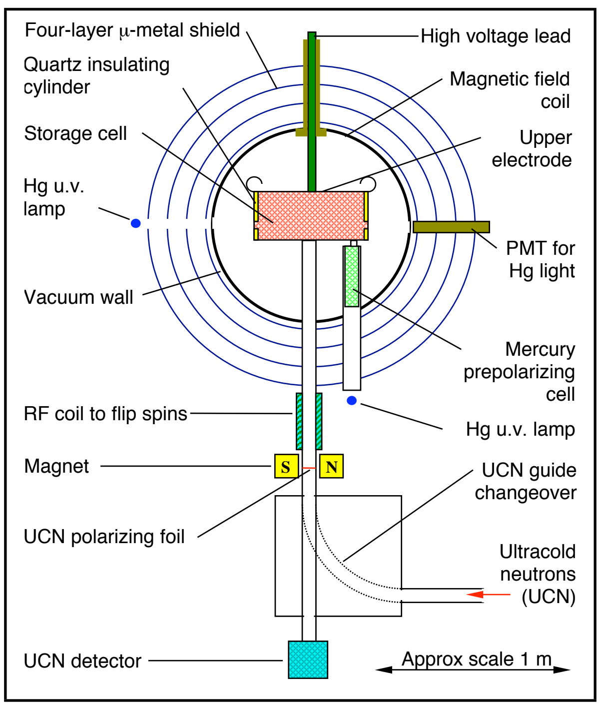

Figure 6: Experimental Apparatus at ILL for most recent nEDM experiment [20].

The current limit placed on the nEDM is from a UCN based experiment at the Institut Laue-Langevin in Grenoble, France. Their apparatus is shown in Figure 6. Their experiment concluded in 2006 with a resulting upper limit of $d_n < 2.9 \times 10^{-26}$ $e\ cm$ (90% C. L.) [20].

Cryo-nEDM depends upon separate cells for the Ramsey oscillation and neutron detection. As shown in Figure 6, The UCNs enter the cell for the Ramsey oscillation where the magnetic field is monitored by ^{199}Hg. However, after the set period of time precessing, the neutrons must be transported out of the magnetic shielding and into a ~~separate~~ polarized ^{3}He detector to measure the number of neutrons in the proper spin state. This provides a possibility for increased errors due to stray electric and magnetic fields.

The experiment had a few dominant systematic errors from electric and magnetic field stability and a $v \times E$ effect which can generate a false EDM. ~~One area where they were particularly hampered was the use of mercury as a co-magnetometer.~~

They used gaseous ^{199}Hg to continually monitor the magnetic field in the cell. The mercury atoms experienced the same magnetic field as the neutrons, so with a precise knowledge of their Larmor frequency, a direct measurement of the magnetic field can be made. Figure 8 shows how the ^{199}Hg correction adjusts the measured resonant frequency of the neutrons.

Knowing the mercury precession frequency, Equation 8 shows how ~~to calculate~~ a measured dipole moment.

$$\frac{\nu_n}{\nu_{Hg}} = \left|\frac{\gamma_n}{\gamma_{Hg}}\right| + \frac{(d_n + |\gamma_n/\gamma_{Hg}|\, d_{Hg})}{\nu_{Hg}} E = \left|\frac{\gamma_n}{\gamma_{Hg}}\right| + \frac{d_{meas}}{\nu_{Hg}} E \tag{8}$$

Since the EDM of ^{199}Hg, d_{Hg} is known to be $(-1.06 \pm 0.49 \pm 0.40) \times 10^{-28}$ e cm [21], this introduces a new systematic error to the experiment. A linear fit is then performed between d_{meas} and the ratio ν_n/ν_{Hg}. A sample of this is shown in Figure 7.

Problems with the ^{199}Hg co-magnetometer method became apparent during the course of the experiment. Most notably is the introduction of a geometric phase due to a gradient in the magnetic field in the presence of an electric field. The mercury atoms are more susceptible to this problem and so the use of a ^{199}Hg co-magnetometer becomes less desirable. Future experiments at ILL will use Superconducting Quantum Interference Devices (SQUIDS) to monitor very small fluctuations in the magnetic fields.

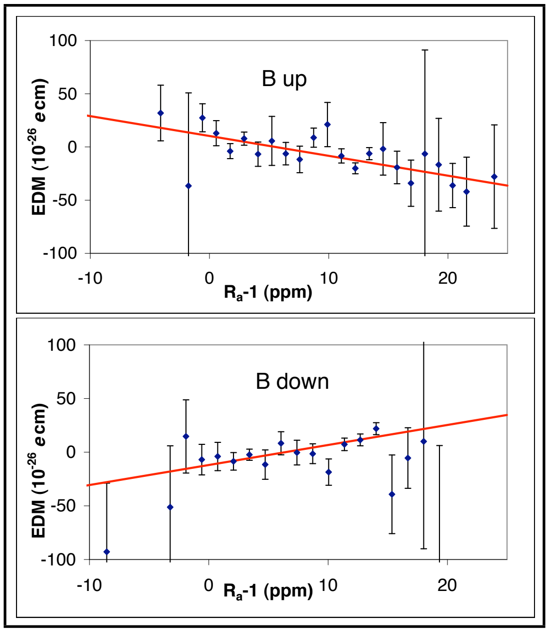

Figure 7: Data from Cryo-nEDM showing a linear fit between a measured EDM and the relative frequency shift between ^{199}Hg and the neutrons[20]

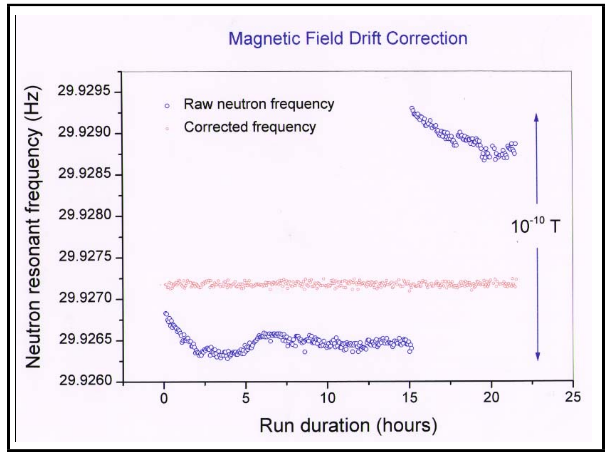

Figure 8: Data from the recent ILL nEDM Experiment. The Blue circles are the measured nEDM values from the neutron resonant frequency. The Red circles are the values after being corrected for magnetic field fluctuations [22, 23].

3.2.2 nEDM at the Spallation Neutron Source, Oak Ridge, Tennessee

The SNS search for the nEDM is currently in the research and development stage. The experiment will be an offshoot of the Fundamental Neutron Physics Beamline. A new building, shown in Figure 9, is being constructed to house the experiment. Construction should be finished in early 2010. Cold neutrons, approximately 8.9 Ångstrom wavelength, enter from the main building at SNS. The neutrons are then passed into the measurement cell, which is filled with high purity liquid ^{4}He. The neutrons down-scatter in the helium through phonon exchange, causing them to cool even further, becoming UCNs. According to the experiment's pre-proposal, the UCN production rate at SNS is estimated to be about 1 UCN/cc/sec [24].

Side and top cutaway views of the apparatus can be seen in Figures 10 and 11. There are two measurement cells, colored blue in the diagram, which will contain the ^{4}He and the UCNs. The cells are surrounded by High Voltage electrodes. The middle plate is the +HV while the exterior plates will be ground. The purpose of the two cells is to provide both positive and negative High Voltage gradient measurements, thereby eliminating certain systematic errors. This is an improvement

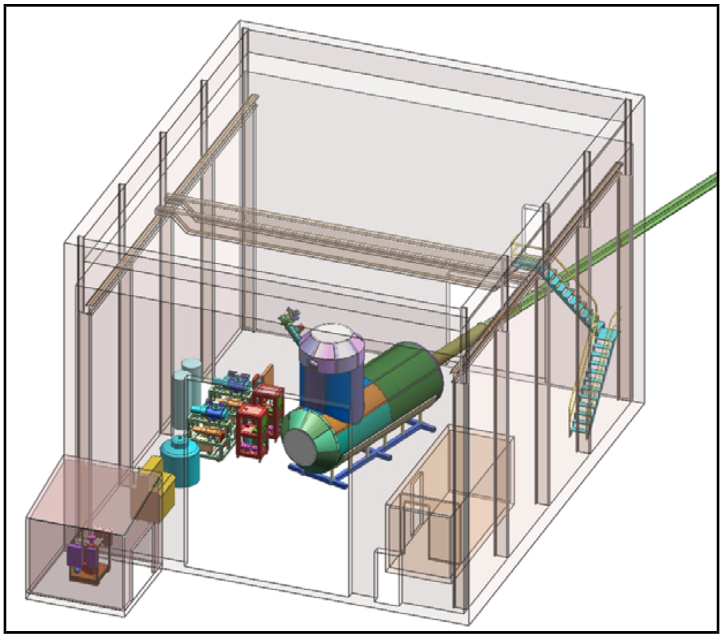

Figure 9: Design of the nEDM Building at the SNS [24].

over the experiment at ILL. The polarity of the electric field ~~is~~ periodically swapped between the two cells, allowing a measurement of when the electric and magnetic fields are both aligned and anti-aligned.

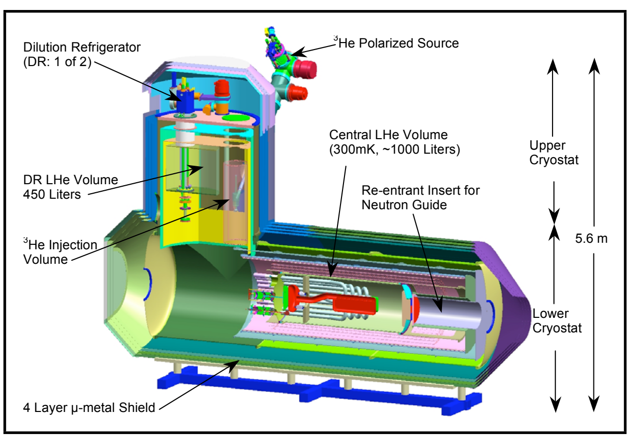

Figure 10: Side view of the Measurement Cell [24].

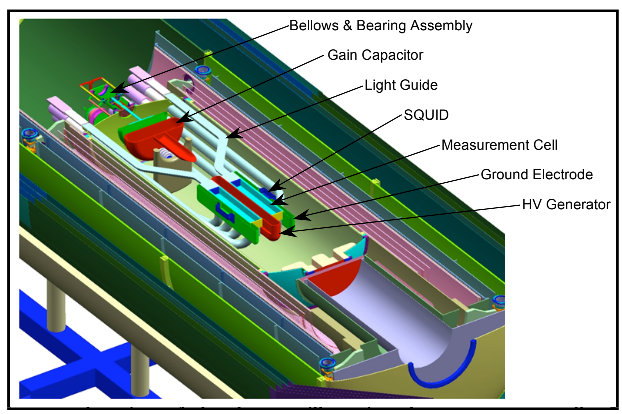

Figure 11: Cutaway view of the Measurement Cell [24].

There will also be a controlled concentration of polarized ^{3}He ~~in~~ the cells. This will act as both a continual measure of the population of UCNs and a co-magetometer for neutrons. This approach has a number of merits over the separate use of a ^{3}He detector and a mercury co-magnetometer.

First, ^{3}He is known to have a significantly smaller EDM than ^{199}Hg. Mercury has a measured EDM that is the same magnitude as the sensitivity of current nEDM experiments, making it sizable a contribution to systematic uncertainties [21]. ~~Conversely, helium has been shown to have an EDM that is significantly smaller than that of mercury. This is d~~ue to the Z^2 dependence of $\vec{d}$ [25].

Secondly, ~~^{3}He and~~ neutrons have a spin dependent capture cross section. The cross section when the spins are anti-aligned is roughly 5000 times larger than when the spins are aligned. Thus the capture rate is dominated by anti-aligned pairs. When the neutron captures with the helium it undergoes the following process:

$$n \; + \; ^3He \rightarrow t + p + 762 \text{ keV}. \tag{9}$$

The 762 keV is an energetic gamma ray that scintillates in the liquid helium. Unfortunately, the scintillation light is in the Ultra-Violet, ~~so it must be converted to visible light through the use of tetra-phenyl butadiene (TPB).~~ The visible light is the signal that is measured.

The measurement procedure, which modifies the Ramsey Method of Separated Oscillatory Fields, is as follows [22]:

1. Polarized ^{3}He, spin up in the z direction, is diffused into the measurement cell containing liquid ^{4}He

2. Cold neutrons pass through a thin foil which polarizes the neutrons to be spin up in the z direction

3. The polarized neutrons then flow into the cells, where they down-scatter in the Superfluid Liquid ^{4}He, at about .5 K, and become UCNs

4. A $\pi/2$ pulse is applied to the cells, which flips the spin of both the ^{3}He and the UCNs into the $x - y$ plane.

5. A weak magnetic field and a strong electric field are applied in the z direction, such that both the ^{3}He and the UCNs precess. A nonzero nEDM, when in an electric field, will cause a shift

in the neutron precession frequency of

$$\Delta\nu = \frac{4d_n E_0}{h}, \tag{10}$$

where d_n is the nEDM, E_0 is the electric field gradient in kV/cm and h is Planck's constant.

6. ~~As the two particles~~, which have slightly different Larmor frequencies, precess, they become increasingly out of phase. At some point, ~~the two~~ will be anti-aligned, and ~~they~~ will capture ~~releasing a 762 keV gamma~~. There will be a beat frequency in the output that is proportional to the difference between the Larmor frequencies of the ^{3}He and the neutrons.

7. ~~The gamma~~ scintillates, ~~creating~~ UV photons that are converted to visible light by TPB. The visible light is then transported via light guides, shown in Figure 11, to photomultiplier tubes.

8. Since the storage time of the neutrons is comparable to the neutron lifetime, 885 s, the remaining helium and neutrons are flushed after 500 s and the whole procedure is repeated.

The signal read out by the tubes over one run will look like an oscillating signal with a decaying amplitude on a decaying background. This background is caused by neutron β decay, which also produces light. The task will be to measure a difference between the $E = 0$ oscillation frequency and the measured $E \neq 0$ frequency. The frequency without an electric field is around 3 Hz, while the Δf that is desired to be measured is order μHz. So the measurement ~~is looking for~~ one part in 10^6. For a further discussion, see nEDM Experiment Pre-proprosal document, reference [24].

4 Simulation as a Method for Determining the Sensitivity of the Oak Ridge nEDM Experiment

Due to the large scale nature of both the design and the cost of current nEDM experiments, it is of great importance to show an experiment's potential sensitivity. It also provides the experiment with help in directing research and development goals. If a simulation shows that certain improvements will greatly impact the overall sensitivity, more effort can be focused on that area. This has been of major importance to the SNS nEDM Collaboration.

4.1 Method of Simulation

For this experiment, we developed a method to simulate data, and then perform the actual analysis. The data stream expected from the real experiment is a series of time stamps when a light pulse is recorded. This pulse comes from the capture on a neutron on $^3He.$ The light output rate can be expressed analytically as [24]:

$$\Phi = \Phi_B(t) + Ne^{-\Gamma_{avg}t}\left[\frac{1}{\tau_\beta} + \frac{1}{\tau_3}\left[1 - P_3 P_n e^{-\Gamma_p t} cos(\omega_r t + \phi)\right]\right], \tag{11}$$

where

$$\Gamma_{avg} = \frac{1}{\tau_\beta} + \frac{1}{\tau_{cell}} + \frac{1}{\tau_3}. \tag{12}$$

The rate equation includes a potentially time-dependent background, $\Phi_B(t)$, which is due to ~~isotropic~~ scintillation from cosmic rays and possible activation from ~~filling~~. Γ_{avg} is the average loss rate of UCN due to beta decay, cell loss and ^{3}He absorption. The P_n and P_3 are the polarization of the UCNs and the ^3He, with $P = 0$ being completely unpolarized (50% up and 50% down) and $P = 1$ being completely polarized. Γ_p is the spin relaxation rate. Finally, ϕ is a phase shift and ω_r is the beat frequency between the neutron and ^{3}He precession:

$$\omega_r = |\nu_3 - \nu_n| \approx 0.3\text{Hz}\,. \tag{13}$$

This is the base frequency for the light output. A non-zero nEDM provides a frequency shift shown in Equation ~~10. Thus~~ resulting in a frequency of:

$$\omega_r^{'} = |\nu_3 - \nu_n| + \frac{4d_n E_0}{h}\,. \tag{14}$$

Using a reasonable (approximately the desired level of sensitivity) value for the nEDM of $6 \times 10^{-26} e\,cm,$ along with the design value for the electric field, 50 kV/cm, yields a frequency shift of:

$$\Delta\nu \approx 2.9\,\mu\text{Hz}. \tag{15}$$

Using the full equation, we can use a Monte Carlo method of generating random times ~~and filling under the curve.~~ The times are sorted and then sent into an analysis code, which does a Maximum Log Likelihood fit to extract both a frequency and a phase. These two values are then compared to input values. A sample run is shown in Figure 12.

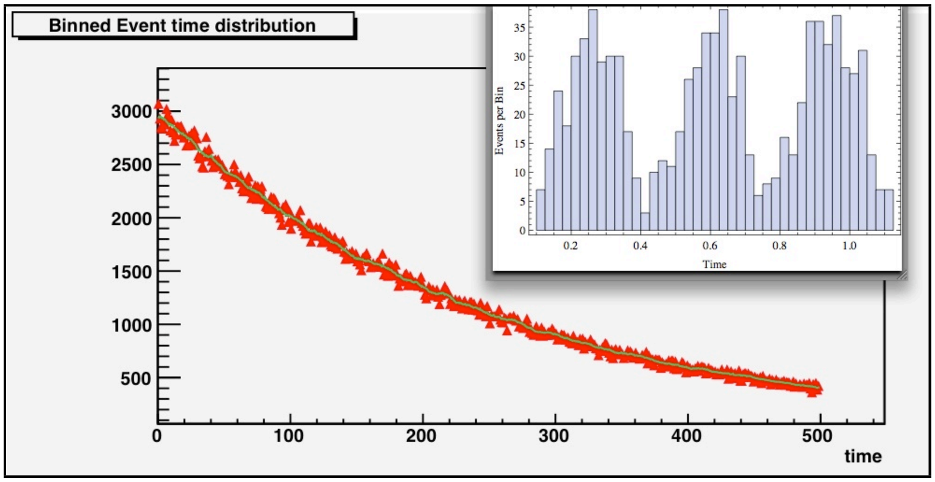

Figure 12: Binned time stamps from a single 500 s run. The main figure is with 1-seccond bins, while the inset is with 0.025-seccond bins.

The data here have been binned in 1-second bins, such that the ≈ 0.3 Hz oscillations are not seen in the full scale. The inset is binned in 0.025-second bins, allowing the oscillations to be seen. This is for visualization only. The data are not binned in the analysis, ~~avoiding problems stemming from binning~~.

After extracting the frequency and phase from a single run, the process is repeated. Typically, approximately 1000 cycles are simulated and then ~~a~~ histogram of the frequency and phase values is generated. The histograms are then fit by a Gaussian, with the centroid ~~being~~ compared to the input values. An example of the frequency histogram is given in Figure 13. Note that the mean value is $2.7 \pm \cancel{.1}\mu$Hz, to be compared with the input value of 2.9μHz.

4.2 Use of Simulation for Optimizing Free Parameters

The example histogram in Figure 13 utilizes the proposed set of research and development parameters, such as cell loss rate, polarization of both the ^{3}He and the neutrons etc. ~~We have been able~~

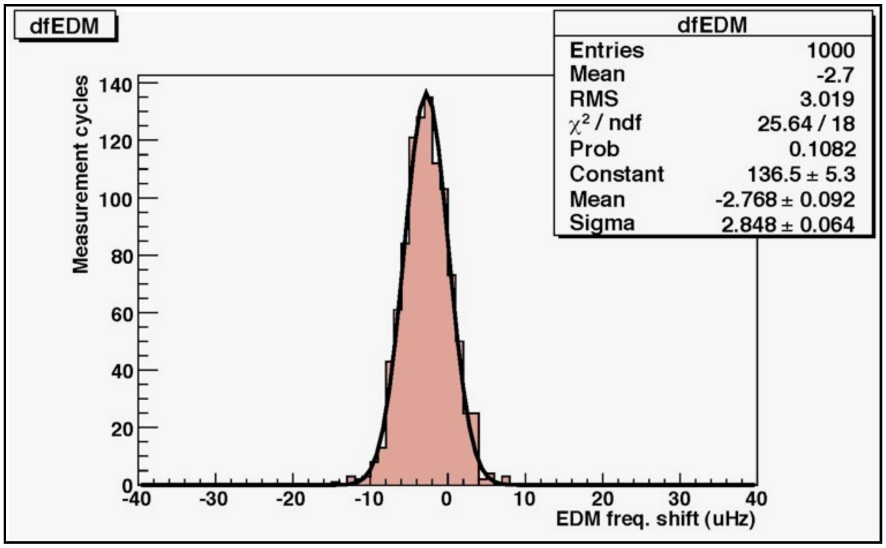

Figure 13: Histogram of the frequency shift due an input nEDM of $6 \times 10^{-26} e\,cm$.

~~to take the achieved values for these parameters and run the simulation. This tool has been used to optimize certain variables, most notably the length of each run.~~

Using the same set of parameters but varying the length of a single run, we can see how the final sensitivity depends upon the measurement time. Figure 14 shows the uncertainty in one run for a given length of measurement cycle. Combining this with the total number of runs gives a measure of the total uncertainty for the experiment, thus enabling an optimizing choice of the length of the run.

This work has been helpful in optimizing certain free parameters, such as the runtime. It will also provide a nice check of the data analysis method well before any "real" data arrives. Any flaws in the analysis method will be worked out with the simulated data.

5 Conclusion

The search for the Neutron Electric Dipole Moment has been one of the longest standing continuous measurements of modern nuclear physics. Over the past 50 years, experiments have pushed down the upper limit over six orders of magnitude. It has become one of the leading tests of physics beyond the Standard Model and will continue to place strict restrictions of new theories.

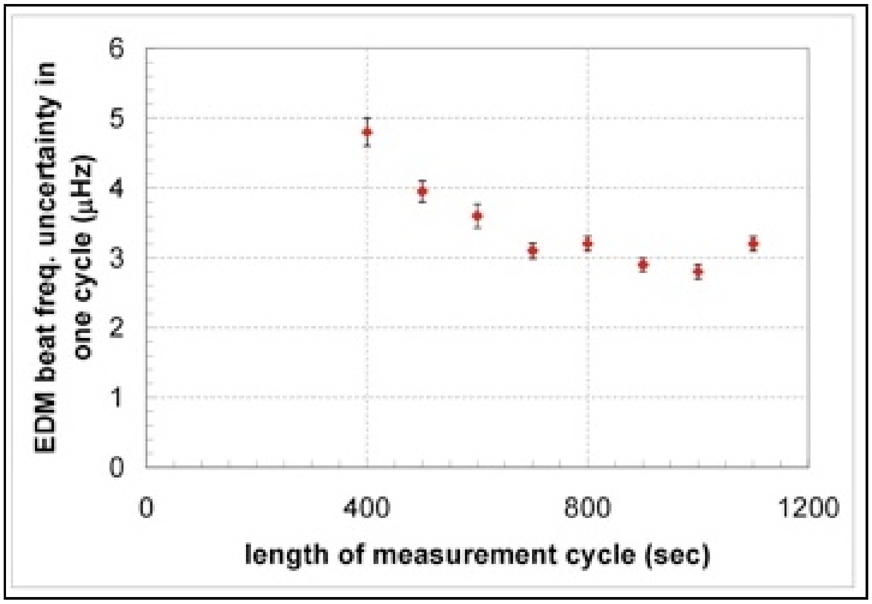

Figure 14: Demonstration of how the uncertainty varies with the length of a single run.

The use of simulated data to determine the overall sensitivity of the experiment has been of great use to the collaboration. It has helped to guide research and development efforts to focus on areas which will provide greatest impact to the sensitivity. It has also been used to optimize certain free parameters, such as the measurement time.

References

[1] E. M. Purcell and N. F. Ramsey. On the possibility of electric dipole moments for elementary particles and nuclei. *Phys. Rev.*, 78(6):807, Jun 1950.

[2] David Griffiths. *Introduction to Elementary Particles*. John Wiley and Sons, Inc., 1987.

[3] Jeffrey S. Nico and W. Michael Snow. Experiments in Fundamental Neutron Physics. *Ann. Rev. Nucl. Part. Sci.*, 55:27–69, 2005.

[4] A. D. Sakharov. Violation of CP Invariance, c Asymmetry, and Baryon Asymmetry of the Universe. *Pisma Zh. Eksp. Teor. Fiz.*, 5:32–35, 1967.

[5] James W. Cronin. CP symmetry violation-the search for its origin. *Rev. Mod. Phys.*, 53(3):373–383, Jul 1981.

[6] I. B. Khriplovich and S. K. Lamoreaux. *CP Violation without Strangness: Electric Dipole Moments of Particles, Atoms and Molecules*. Springer, 1997.

[7] Shahida Dar. The neutron EDM in the SM: A review. 2000.

[8] Cheng Ta Pei and Li Ling Fong. *Gauge Theory of Elementary Particle Physics*. Clarendon Press, Oxford, 1984.

[9] Samuel S M Wong. *Introductory nuclear physics; 3rd ed.* Wiley, New York, NY, 1998.

[10] Yue Zhang, Haipeng An, Xiangdong Ji, and Rabindra N. Mohapatra. General CP Violation in Minimal Left-Right Symmetric Model and Constraints on the Right-Handed Scale. *Nucl. Phys.*, B802:247–279, 2008.

[11] Rabindra N. Mohapatra and Jogesh C. Pati. Left-right gauge symmetry and an “isoconjugate” model of *cp* violation. *Phys. Rev. D*, 11(3):566–571, Feb 1975.

[12] Tarek Ibrahim and Pran Nath. Neutron and electron electric dipole moment in $n = 1$ supergravity unification. *Phys. Rev. D*, 57(1):478–488, Jan 1998.

[13] T. D. Lee and C. N. Yang. Question of parity conservation in weak interactions. *Phys. Rev.*, 104(1):254–258, Oct 1956.

[14] C. S. Wu, E. Ambler, R. W. Hayward, D. D. Hoppes, and R. P. Hudson. Experimental test of parity conservation in beta decay. *Phys. Rev.*, 105(4):1413–1415, Feb 1957.

[15] J. H. Smith, E. M. Purcell, and N. F. Ramsey. Experimental limit to the electric dipole moment of the neutron. *Phys. Rev.*, 108(1):120–122, Oct 1957.

[16] Ya. B. Zel'dovich. Cold neutron storage. *Zhur. Eksptl'. i Teoret. Fiz.*, 36:1952 – 1953, June 1959.

[17] A. P. Serebrov, V. E. Varlamov, A. G. Kharitonov, A. K. Fomin, Yu. N. Pokotilovski, P. Geltenbort, I. A. Krasnoschekova, M. S. Lasakov, R. R. Taldaev, A. V. Vassiljev, and O. M. Zherebtsov. Neutron lifetime measurements using gravitationally trapped ultracold neutrons. *Physical Review C (Nuclear Physics)*, 78(3):035505, 2008.

[18] C. M. O'Shaughnessy et al. Measuring the Neutron Lifetime Using Magnetically Trapped Neutrons. 2009.

[19] J. S. Nico et al. Observation of the radiative decay mode of the free neutron. *Nature*, 444:1059–1062, 2006.

[20] C. A. Baker, D. D. Doyle, P. Geltenbort, K. Green, M. G. D. van der Grinten, P. G. Harris, P. Iaydjiev, S. N. Ivanov, D. J. R. May, J. M. Pendlebury, J. D. Richardson, D. Shiers, and K. F. Smith. Improved experimental limit on the electric dipole moment of the neutron. *Physical Review Letters*, 97(13):131801, 2006.

[21] M. V. Romalis, W. C. Griffith, J. P. Jacobs, and E. N. Fortson. New limit on the permanent electric dipole moment of $199hg$. *Phys. Rev. Lett.*, 86(12):2505–2508, Mar 2001.

[22] nEDM Collaboration. Conceptual design report for the neutron electric dipole moment project (nEDM), February 2007.

[23] P. G. Harris, C. A. Baker, K. Green, P. Iaydjiev, S. Ivanov, D. J. R. May, J. M. Pendlebury, D. Shiers, K. F. Smith, M. van der Grinten, and P. Geltenbort. New experimental limit on the electric dipole moment of the neutron. *Phys. Rev. Lett.*, 82(5):904–907, Feb 1999.

[24] nEDM Collaboration. A new search for the neutron electric dipole moment: Funding pre-proprosal, March 2002.

[25] V. A. Dzuba, V. V. Flambaum, and J. S. M. Ginges. Atomic electric dipole moments of he and yb induced by nuclear schiff moments. *Physical Review A (Atomic, Molecular, and Optical Physics)*, 76(3):034501, 2007.